Pre-print.

El artículo fue aceptado para publicación y fue publicado

Editorial: Wiley Online Library

DOI: https://doi.org/10.1002/jsfa.9307

Rodríguez-López, M.I., Mercader-Ros, M.T., López-Miranda, S., Pellicer, J.A., Pérez-Garrido, A., Pérez-Sánchez, H., Núñez-Delicado, E., Gabaldón, J.A. (2019). Thorough characterization and stability of HP-***β***-cyclodextrin thymol inclusion complexes prepared by microwave technology: A required approach to a successful application in food. Journal of the Science of Food and Agriculture Disponible. Agriculture 99 (3), 1322-1333.

Thorough characterization of HP-β-Cyclodextrin Thymol inclusion complexes. A required approach to a successful application in food industry

Running Tittle: Characterization of HP-β-Cyclodextrin Thymol inclusion complexes

Isabel Rodríguez-López[1], Teresa Mercader-Ros[1], Santiago López-Miranda[1], José Antonio Pellicer[1], Alfonso Pérez-Garrido[2], Horacio Pérez-Sánchez[2], Estrella Núñez-Delicado[1], José Antonio Gabaldón[1]*

[1] UCAM Universidad Católica de Murcia. Department of Food Technology and Nutrition. Molecular Recognition and Encapsulation Group (REM). Avenida de los Jerónimos s/n. 30107 Guadalupe. Murcia. Spain.

[2] UCAM Universidad Católica de Murcia. Department of Degree in Computer Science. Bioinformatics and High Performance Computing Group (BIO-HPC). Avenida de los Jerónimos s/n. 30107 Guadalupe. Murcia. Spain.

*Corresponding author: José Antonio Gabaldón Hernández

Telf: +34 968 278622

e-mail: jagabaldon@ucam.edu

UCAM Universidad Católica de Murcia. Department of Food Technology and Nutrition. Avenida de los Jerónimos s/n 30107 Guadalupe, Murcia, Spain.

ABSTRACT

BACKGROUND

The aim of the present study was to obtain a stable dry powder formulation of cyclodextrins (CDs) encapsulating thymol, for a successful application as an ingredient at industrial scale, as well as, to characterize the thymol-CDs complexes by different techniques.

RESULTS

Thymol was successfully solubilized in aqueous solutions and the Kc value increased with the pH of the media until neutral pH, obtaining the highest values (2583 ± 176 L mol^{-1}) for HP-β-cyclodextrins (HP-β-CDs). The best encapsulation efficiency of thymol in solid complexes was obtained using the microwave (MWI) encapsulation method. The different characterization techniques have demonstrated the affinity of HP-β-CDs to thymol molecules, forming stable complexes.

CONCLUSIONS

The results obtained support the use of the MWI method in the preparation of solid HP-β-CD-thymol complexes, due to the greater encapsulation efficiency and technological and economic advantages for industrial applications.

Keywords

Encapsulation, Thymol, HP-β-CDs, spray-drying, microwave irradiation.

INTRODUCTION

Essential oils (EOs) are volatile and un-colored fluids, easily soluble in lipids and organic solvents. These EOs can be obtained from different plant organs such as roots, flowers, stems or leaves, and their components are usually located in secretory and epidermic cells or glandular trichomes.[1] EOs have a complex composition, containing between 20–60 components at quite different concentrations. Two or three compounds are major components at fairly high concentrations compared to others present in trace amounts.[2] Thymol (2-isopropyl-5-methylphenol), is the major component of the *Origanum* and thyme essential oils, and is the responsible for relevant biological properties of these EOs. In fact, despite having recently received a growing attention as natural biocides, due to their potent activity against a broad range of natural spoilage bacteria, fungi and foodborne pathogens, we found in the literature numerous works focused on the demonstration of their health benefits as antimutagenic, anticancer, antiviral, anti-oxidant, anti-diabetic and anti-inflammatory.[3-10] These properties are due to the presence of their major components, which have a low molecular weight and a high volatility.

Thymol is the most abundant compound of the essential oils from plants belonging to the *Lamiaceae* family.[11-13] It has been demonstrated that this phenol has a remarkable antioxidant and anti-inflammatory activity and it is sometimes prescribed as a local anesthetic, contraceptive, healing and antiseptic. In addition, it has antibacterial and antifungal activity, as well as beneficial effects on the cardiovascular system.[14] Different mechanisms of action by which thymol exerts protective effects against cancer have been proposed, as it is able to inhibit cell growth,[15] induce independent and caspase-dependent apoptosis,[16-18] and also the depolarization of mitochondrial membrane.[19]

Given the benefits described for thymol in different sectors such as food or agriculture, as well as medicine or pharmacy, it would be interesting developing strategies allowing to solve the drawbacks derived from its physicochemical properties, which restrict its widespread use, such as its low aqueous solubility, its relatively high flavor impact and instability to different environmental factors such as temperature, light and oxygen.

In order to solve these drawbacks, the use of different encapsulation techniques has been proposed. Thus, several articles in the literature have focused on the employ of encapsulation technologies for EOs or different components of EOs, including molecular inclusion with host molecules, such as starch,[20] arabic gum,[21] cellulose and polyvinyl-pyrrolidone,[22] chitosan and angicgum,[23-24] liposomes[25-26] and cyclodextrins.[27]

Despite that several studies attempted to preserve thymol by cyclodextrins, usually only the formation constant (Kc) of the inclusion complexes has been reported, since complexation was a previous step to achieve another main goal, the experimental evidence of a relevant thymol property.[18,22,24] In this sense, information on different encapsulation methods to maximize thymol concentration in the complex and its stability over time is scarce.

Thus, for a successful application as ingredient at industrial scale, producing a standardized dry powder formulation of cyclodextrins encapsulating a volatile and poorly water-soluble molecule is a key challenge, since thymol can leak out during spray drying or storage steps. To the best of our knowledge, this approach has not been yet investigated.

Therefore, the present study aimed to optimize a basic work methodology for standardization of the encapsulation process with different CDs types, selecting thymol as model compound, as well as a thorough characterization of the solid complexes by

^{1}HNMR, Fourier transform infrared spectroscopy (FT-IR) and differential scanning calorimetry (DSC) techniques, to evidence the inclusion of thymol into the CDs hydrophobic cavity. In addition, the strength of interactions, geometry, structural aspects and energetically favorable conformation for inclusion complexes formation by applying scanning electron microscopy (SEM) and molecular docking were explored.

EXPERIMENTALS

Reagents and standards

Thymol (99 % purity) was purchased from Sigma (Madrid, Spain). The α- β- and HP-β-CDs were supplied by AraChem (Eindhoven, Holland). Others chemical reagents used were of analytical grade.

Solubility studies

The complexation process of thymol in CDs was evaluated by developing phase solubility diagrams, according to the method described by Higuchi and Connors, with some modifications.[28] Excess amounts of thymol were added to 5 mL of aqueous solutions of increasing concentrations of CDs from 0 to 10 mmol L^{-1} for β-CDs, 0 to 50 mmol L^{-1} for α-CDs and 0 to 100 mmol L^{-1} for HP-β-CDs. The different phase solubility diagrams were prepared in glass test tubes and maintained in an ultrasonic bath (Ultrasons H.P., Selecta, Spain) for 60 min and 25 ºC, to reach equilibrium.

The effect of pH on the complexation process was studied by developing solubility diagrams in buffer solutions of CDs at pH 3.5, 5.5 (sodium acetate buffer 100 mmol L^{-1}), 6.5, 7.0 (sodium phosphate buffer mmol L^{-1}) and pH 8.5 (sodium borate buffer 100 mmol L^{-1}).

After 60 min in ultrasound bath, solutions were filtered using 0.45 μm nylon membrane filters to eliminate thymol excess (Chromafil, Macherey-Nagel, Germany). Prior to quantification by GC-MS of thymol content of the complexes in filtered solutions, they were diluted in ethanol (solution:Ethanol, 20:80,v:v). Phase solubility diagrams were carried out in triplicate.

Complexation by using microway as energy source (MWI)

Complexes between HP-β-CDs and thymol were formed by using MWI, as described by Hernández-Sánchez.[29] Solutions of HP-β-CDs (100 mL, from 0 to 100 mmol L^{-1}) were irradiated in a microwave oven (LG Grill Wavedom, LG Electronics Las Rozas, Spain), at 700 W for 30 s at 10 s intervals to reach 70 ºC. Excess of thymol was then added to the HP-β-CDs solutions, which were irradiated again for 30 s at 10 s intervals to reach 70 ºC. Then, the samples were stirred and kept overnight in sealed vials in darkness, at 25 ºC, before being divided in two groups. The first one was filtered using 0.45 μm nylon membrane filters (Chromafil, Macherey-Nagel, Germany) (24h MWI), while the second group was subjected again to the same process 12 hours later (MWI up to 70 ºC, 12 h in darkness and filtration) (48 h MWI). Prior to quantification of thymol content of the filtered samples by GC-MS, they were diluted in ethanol (solution:Ethanol, 20:80,v:v). Phase solubility diagrams were made in triplicate.

Quantification of thymol by GC-MS analysis

The quantification of thymol was carried out by GC-MS analysis. A Shimadzu GC-QP 2010 (Kyoto, Japan) gas chromatographer was used. The GC was combined with a mass spectrometer. Helium was used as carrier gas, at a flow rate of 0.5 mL min^{-1}. Aω-WAX 250 fused silica supelco column (30 m x 0.25 mm x 0.25 μm thickness), was used.

171 The conditions of temperature were as follows: initial temperature at 70 ºC, raised to 160
172 ºC at 4 ºCmin^{-1}, raised to 280 ºC at 30 ºCmin^{-1}, and maintained finally at 280 ºC for 6
173 min. Injector temperature was 250 ºC and injector mode was Split 1:20.

174 The peak area of each sample was used for thymol quantification (mmol L^{-1}), by
175 interpolating in the calibration curve obtained using a standard of thymol, defined by
176 equation: Area = 7544.4+1.80·10^6 [thymol (mmolL^{-1})] and (R^2 = 0.9968) for thymol
177 concentration from 0 to 0.5 mmol L^{-1}.

178

179 **Complexation constant calculation (k_C) and complexation efficiency (CE)**

180 Kc between thymol and CDs was calculated from the slope of the phase solubility
181 profile and the solubility of thymol in aqueous solution (S_0) by using the equation (1):

182 $$K_C\,(L{\cdot}mol^{-1}) = \frac{slope}{S_o{\cdot}(1-slope)} \qquad (1)$$

183 CE is the ratio between dissolved complex and free CDs concentration. It is
184 independent of S_0, and was calculated from the slope of the phase solubility profiles by
185 using the equation (2).

186 $$CE(\%) = \frac{[disolved-complex]}{[CD]_f} = S_0 * K_C * 100 \qquad (2)$$

187 The molar ratio thymol:CD, was calculated using CE values with equation (3).

188 $$\text{thymol:CD} = \frac{1}{\left(1+\frac{1}{CE}\right)} \qquad (3)$$

189

190 **Spray dry and stability of dehydrated complexes**

191 The HP-β-CD-thymol solid complexes were obtained by spray dry. The spray
192 dryer used was a Buchi B-290 device (Flawil, Switzerland). The functional parameters of
193 the spray drier were as follows: inlet air temperature 170 ºC, outlet air temperature 68 ºC,

194 35 $m^3 h^{-1}$ of inlet air flow, 5 mL $min^{-1}$of pump flow and 360 L h^{-1} of compressed air
195 caudal. The recovered powder was stored in an airtight glass container prior to
196 analysis.The solid complexes were stored in airtight sealed glass tubes at 25 ºC and 4 ºC.
197 The drying process yield was calculated using equation (4):
198 $$Dryingprocessyield = \frac{\text{dehydrated complexes obtained (g)}}{\text{total solids in solution (kg)}} \quad (4)$$
199 The encapsulation yield was calculated using equation (5):
200 $$Thymol\ yield = \frac{\text{total thymol in dehydrated complexes (g)}}{\text{total thymol in disolved complexes (kg)}} \quad (5)$$
201 Prior to quantification of thymol content in the dehydrated complexes by GC-MS,
202 solid complexes were diluted in water (Complex:Water, 1:1,w:v) and filtered using 0.45
203 μm nylon membrane filters (Chromafil, Macherey-Nagel, Germany). Then, dissolved
204 complexes were diluted in ethanol (Complex:Ethanol, 20:80,v:v). Quantification of
205 thymol content in dehydrated complexes was made in triplicate.
206 The stability of the of dehydrated HP-β-CD-thymol complexes was studied by
207 measuring the thymol content in the dehydrated samples during 17 months, maintained
208 at two different temperatures,4 ºC and 25 ºC. Samples were analyzed by triplicate.
209
210 **^{1}H and 2D NMR spectroscopy**
211 H-NMR spectra of thymol, CDs, and the inclusion complexes (dissolved in D_2O)
212 were recorded on a 600 MHz spectrometer (Bruker Avance, Germany) at 25 °C. Chemical
213 shifts given in parts per million (ppm), are relative to a tetramethyl silane internal standard
214 (δ=0.0), and NMR data were processed with MestReNova software (6.0.2-5475 version).
215 Two dimensional rotational frame nuclear Overhauser effect spectroscopy (2D ROESY)
216 spectra using the standard Bruker pulse program roesygpph were acquired at 32 scans, an
217 acquisition time of 0.150 s and a pulse delay of 2.3 s.
218

Fourier transform infrared spectroscopy (FT-IR)

The Fourier transform infrared spectroscopy (FTIR) spectra used to study changes of chemical structures of free thymol, and thymol complex were acquired using a Varian FT-IR 670 (Agilent Tech., the Netherlands) spectrophotometer coupled with an accessory to analyze the attenuated total reflectance (ATR) with a wave number resolution of 0.10 cm^{-1} in the range of 250–4,000 cm^{-1}. A minimum of 32 scans were signal-averaged with a resolution of 4 cm^{-1} in the above ranges.

Thermal analyses

The thermal transitions of the isolated and complexed components were recorded by differential scanning calorimetry (DSC), using an analyzer Mettler DSC Q100 (TA Instrument, Cerdanyola del Valles, Spain). Samples of thymol, HP- β-CDs, and thymol complexes were weighed to the nearest 0.1 mg into aluminium capsule and sealed. For the performance of the test, 4-5 mg of sample were weighed into aluminum capsules, which were taken to Hi-Res TGA 2950 thermogravimetric analysis equipment (TA Instrument, Cerdanyola del Valles, Spain), that operated with a scanning rate of 10 °C min^{-1} from 25 ºC to a maximum temperature of 300 °C with nitrogen as the carrier gas. Thermal stability of the respective components is shown using first derivative plots (DTG) of weight (%) against temperature (°C).

Field Emission Scanning Electron Microscope (FESEM) images

The solid complexes were examined under Field Emission Scanning Electron Microscopy (FESEM) using MERLIN™ VP COMPACT (Carl Zeiss Microscopy SL, Germany). The microscopy images were taken using a SE2 detector under an accelerating voltage of 1 kV.

244 **Molecular docking**

245 The molecular structures for thymol and CDs used in this study were built
246 manually using AutoDockTools[30] and structural information derived from experimental
247 data. The structure of β-CDs was extracted from the crystal structure of the Protein Data
248 Bank (PDB) with code 3CGT. The structure of HP-β-CDs model was built by adding
249 hydroxylpropyl groups to the β-CDs model. Molecular docking calculations were carried
250 out using default parameters in AutoDockVina.[31] Hydroxylpropyl groups of HP-β-CDs
251 were explicitly considered as flexible during docking simulations. Graphical
252 representations of the docking results were prepared using PyMOL (Molecular Graphics
253 System, version 1.3, Schrödinger, LLC).

254

255 **Statistical analysis**

256 Data were analysed by using the statistical analysis software SPSS (v.21). Values
257 represent means of triplicate determinations and error bars in figures represent standard
258 deviation.

259

260 **RESULTS AND DISCUSSION**

261 **Complexation of thymol in CDs**

262 In order to study the ability of CDs to increase the aqueous solubility of thymol,
263 phase solubility studies were carried out at different pHs (3.5; 5.5; 6.5; 7.0; 8.5) at 25 ºC
264 with different types of native or modified CDs (α-CDs; β-CDs; HP-β-CDs). The results
265 obtained by using these types of CDs are shown in Figure 1.

266 The phase solubility diagrams of thymol and CDs showed a linear relationship
267 between thymol and CDs concentration, showing A_L type phase solubility diagrams,

which means that the stoichiometry of the inclusion complexes formed were 1:1, in all cases.

Assuming the formation of 1:1 complexes, it was possible to calculate the complexation constant (Kc) and the complexation efficiency (CE) values between thymol and CDs, by using linear regression analysis ofthe phase solubility diagrams according to equations 1 and 2. The Kc value describes the strength of the interaction between thymol and CDs, and can be used to compare the stability of the complexes formed between thymol and each type of CDs. The solubilising effect of CDs is showed by the complexation efficiency (CE). This parameter is independent on S_0,[32] and represents the molar ratio between complex and free CDs concentration.[33] The values of S_0, Kc and CE are shown in Table 1.

The experimental data showed that the Kc value increased with pH until neutral pH. This effect could be due to the fact that the solubility (S_0) of thymol decreased from 6.42 mmol L^{-1} to 5.54 mmol L^{-1} as pH increased from 3.5 to 7.0. However, a slight increase at pH 8.5 (5.92 mmol L^{-1}) was observed. It should be noted that the aromatic structure of thymol (derived from phenol), determines its reactivity, behaving as a weak acid (pKa = 10.62). Therefore, the pH of the medium could conditionits dissociation degree and consequently its solubility.

Being more acidic than water and coming into contact with alkaline hydroxides in aqueous solution at basic pH, thymol reacts with alkaline hydroxides to form salts or phenoxide ions, more stable than thymol itself (at neutral pH), due to the net effect of the resonance of the aromatic ring. The formation of thymol inclusion complexes with CDs determines a decrease in the enthalpy and an increase in the entropy of the system, reducing thus the free energy, which causes an increase in the stability of the complex. Therefore, the protonation of thymol and its solubility are determinants in the complexes

293 stability. Taken into account that the internal cavity of the CD is quite hydrophobic, the
294 inclusion of apolar and uncharged species is favored versus polar hydrated or net charge
295 species, since the inner surface of the cone that will receive the host molecule is apolar.
296 In fact, for the three types of CDs studied (Table 1), a significant increase in complexes
297 stability (Kc values) at pH 7 was observed.

298 In relation to CDs cavity size, the Kc values obtained for native CDs were higher
299 for β- than for α–CDs (Table 1). The size of the hydrophobic cavity of α-CDs (0.49 nm)
300 may be too small, whereas β-CDs (0.62 nm), is more appropriate to accommodate therein
301 the aromatic rings of thymol (Figure 1).

302 With respect to the Kc values, differences observed between β- and HP-β-CDs
303 (1184 ± 115 L $mol^{-1}$and 2583 ± 176L mol^{-1}, respectively), these could be due to the
304 intensity of the hydrophobic forces and van der Waals interactions involved, the release
305 of the ring stress, and to a greater extent, the presence of hydroxypropyl groups in the
306 modified CDs, making the thymol molecules more accessible to the apolar cavity. On the
307 other hand, the hydroxypropyl groups may also cause the opening of the CD cavity,
308 significantly modifying its size with respect to the native CD, thereby favoring the
309 complete thymol molecule inclusion in the internal cavity of the HP-β-CDs, whereas in
310 the case of β-CDs, is only able to penetrate a part of the thymol molecule.

311 However, it is important to note that the value of Kc does not depend only on the
312 increase in the aqueous solubility of thymol when complexed with CDs, but also on the
313 aqueous solubility (S_0) of thymol. Therefore, the efficacy of thymol complexation (CE)
314 and the molar ratio (thymol:CD) for each type of CDs (Table 1), were also determined by
315 using equations (2) and (3).

316 The comparison of CE parameter is more convenient than comparing Kc values
317 when the study involves different types of CDs, or different complexation conditions for

318 the same compound. CE values obtained ranged from 37.8% for α-CDs at pH 7.0 to
319 139.5% for HP-β-CDs at pH 7.0 (Table 1). This high value above 100% indicates that at
320 pH 7.0, there are more HP-β-CDs complexing thymol than free in solution. The values
321 obtained for molar ratio ranged from 1:4 to 1:2, indicating that about one of every 4 or 2
322 CDs molecules in solution is forming soluble complexes whit thymol (Table 1).
323 Comparing the tree types of CDs studied, α-CDs showed lowest CE values and
324 molar ratio (between 1:4 and 1:3) than those obtained for β- or HP-β-CDs. In the case of
325 β- and HP-β-CDs, molar ratio were between 1:3 and 1:2, indicating that in many cases
326 one of every 3 or 2 β- or HP-β-CDs molecules in solution is forming soluble complexes
327 whit thymol.
328 In summary, HP-β-CDs at pH 7.0 showed the highest Kc value (2583 ± 176 L
329 mol^{-1}) and the highest CE (139.5%) for thymol complexation, despite of at this pH,
330 thymol presented its lower aqueous solubility (0.54 ± 11 mmol L^{-1}) (Table 1).
331
332 **Complexes formation optimization**
333 Once the ability of α-, β- and HP-β-CDs to form inclusion complexes with thymol
334 has been demonstrated, HP-β-CDs were selected to optimize the complexes formation
335 because of their higher CE (139.5±12.3%) and Kc (2583 ± 176L mol^{-1}) values at neutral
336 pH (7.0) with respect to the native CDs tested. To optimize the encapsulation of thymol
337 by HP-β-CDs, two encapsulation methods were compared: solubility and microwave
338 irradiation method (MWI) described by Hernández-Sánchez.[29]
339 Figure 2 shows the phase diagrams obtained using the solubility and microwave
340 irradiation methods. Both methods showed that the stoichiometry of the complexes
341 obtained was 1:1, and no difference between the number of microwave cycles applied to
342 the samples (○ 24 h MWI, ● 48 h MWI) were observed. The Kc values obtained by using

one or two microwave cycles were 4835 ± 94 L mol^{-1} and 4696 ± 87 L mol^{-1}, respectively, indicating that a contact time of 24 h and the application of only one microwave cycle were adequate to reach the equilibrium of the mixture. So, the Kc value between thymol and HP-β-CDs used from now on will be the average value 4765 ± 90.5 L mol^{-1}. However, this value of Kc obtained by using MWI method was significantly higher than that obtained by the solubility method (2583 ± 176L mol^{-1}). This result could be due to the fact that microwave irradiation has the ability to penetrate into any substance, causing the rotation of molecules with an electric dipole such us water molecules. In other words, it stimulates the interaction of some molecules with others, favoring the exit of the water molecules from the CDs cavity, a circumstance that takes advantage for the thymol molecules to enter into the empty apolar cavity.[34]

It should be noted that microwave irradiation does not affect the activation energy required to initiate the complexation, but provides almost instantaneously enough energy to overcome this barrier, and complete the reaction more quickly and with greater efficiency than using other methods of energy application. In addition, the energy transmitted by the microwaves affects the temperature parameters described in the Arrhenius equation. As a consequence, this instantaneous heating causes a faster molecular movement (increase of the kinetic energy), generating a greater number of collisions and favoring the dissolution of the different compounds.

Complexes dehydration and stability

Soluble complexes HP-β-CDs-thymol were subjected to a spray drying process to obtain complexes in solid state. This drying method was applied because it is widely used in the food industry, and in addition, there are different studies that corroborate its usefulness in obtaining solid complexes with CDs.[35-37]

368 The structure and size of the solid complexes obtained from the dehydration
369 process were analysed. The analysis of the appearance of the dehydrated structures
370 obtained by scanning electron microscope (SEM) images, showed that the spray dried
371 complexes were composed of irregular particles with spherical shape, revealing numerous
372 folds and dents at the surface (Figure 3 B and C). This geometric shape and variable size
373 is typical of the materials obtained by spraydrying.[38]

374 According to Loksuwan,[39] the folds at the surface of the atomized particles and
375 the expansion of their size, are usually generated as a result of the presence of core
376 materials (CDs), since they slow down the evaporation rate of the system water due to
377 their ability to retain water molecules (Figure 3). As can be seen in Figure 3 (B and C),
378 the outer surfaces of certain complexes show continuous walls, without cracks, which
379 have a significant influence on the retention of volatile compounds.

380 In previous studies some particle morphologies are described, such us
381 microencapsulated coffee oil,[40] oregano essential oil[41] and laurel infusions.[42] In all cases,
382 microparticles with external globular morphology similar to those described in Figure 3
383 were described.

384 The yield of the dry process was also calculated by using Equations 4 and 5, and
385 the results are shown in Figure 4.The drying process yield was higher than 500 g of solid
386 material recuperated by kg of solid material introduced into the spray dryer, but lower
387 than 800 g kg^{-1} in all HP-β-CDs concentration used. At laboratory scale, it is difficult to
388 achieve yields above 800 g kg^{-1},[43] since the quantity of soluble solids are generally small
389 and therefore the proportion of material lost during the drying process is high. At
390 industrial scale, by increasing the working quantities, the drying yield would be higher,
391 with values above 900 g kg^{-1}. The dry process yield (Figure 4A) was dose-dependent,
392 showing higher values as HP-β-CDs concentration increased. The highest dry process

393 yield (766 g kg^{-1}) was obtained for a 100 mmol L^{-1} HP-β-CDs concentration using the
394 solubility method.

395 The dry process yield tended to be higher for the solubility encapsulation method
396 than MWI encapsulation method (Figure 4A). The difference between both methods
397 could be justified considering that for the same CDs concentration; there was a higher
398 quantity of thymol in solution when complexes were formed by MWI, resulting in a
399 higher quantity of solids in the dried mixture, and also increasing the solution viscosity.[38]
400 This fact could provoke a greater adhesion of the dehydrated powder to the wall of the
401 dehydration chamber, increasing the amount of solid complexes lost and reducing the dry
402 process yield.[44]

403 The thymol retention capacity after the dehydration process was evaluated by the
404 thymol yield (Equation 5). The data obtained are shown in Figure 4B. Comparing the
405 thymol yield achieved by drying complexes obtained by both, solubility and MWI
406 methods, it was observed that the values obtained were on average, 28 % higher for the
407 MWI samples. These results could be explained considering that CDs reach an instant
408 state of resonance with the MWI method, and therefore, favoring the exit of water
409 molecules from the CDs cavity, and the input of the thymol molecules.[45]

410

411 **Stability of solid complexes**

412 The stability of solid complexes was also studied, evaluating the content of thymol
413 in the powder with the storage time, at different temperatures. As it is shown in Figure 5,
414 the solid complexes coming from MWI tend to retain more effectively the thymol (Figure
415 5, B). When the storage temperature was 25 °C, the thymol losses at 17 months of storage
416 was 20% in the case of MWI complexes (Figure 5B, ●), whereas it was more than 50%
417 in the case of solubility method complexes (Figure 5A, ●).

When the storage temperature was 4 ºC, HP-β-CDs-thymol complexes obtained by MWI were able to avoid the losses of thymol until the fourth month of storage, although from that moment, the losses increased in a significant way reaching a loss percentage of 75% at 17 months. It was also observed that the conservation of the complexes at a low temperature (4 ºC) increased the losses of thymol in a more pronounced way than at 25 ºC. These results can be justified considering that, by storing the samples at a lower temperature, the moisture content in the surrounding environment increases considerably, favoring an unequal competition between the thymol and water molecules for the CDs internal cavity (hygroscopic molecules), causing the release of the thymol complexed.

These results agree with those previously described by Mohit,[46] for the complexation of cefdinir with β-CDs by MWI and subsequent atomization.

Nuclear magnetic resonance (NMR)

^{1}H NMR spectra of thymol, HP-β-CDs, and the inclusion complexes (dissolved in D_2O) were obtained. Thymol was really included inside the lipophilic HP-β-CDs cavity. Other techniques like DSC, IR, UV-Vis, are able to either suggest or establish if the guest molecules form a complex or not, but they are unable to give any sure finding, neither on the kind of complex (if inclusion or adsorption) nor on the structural conformation of the molecules.[20] Analyzing data obtained from ^{1}H-NMR experiments it was possible to define the stoichiometry of the complexes: for either thymol the ratio was 1:1. Table 2 reportsthe chemical shift values of thymol and HP-β-CDs protons (Figure 1 A-B), in the free and complex state in D_2O solution, as well as the differences between the signals of the free and included molecules.

Besides, it is well known that two-dimensional (2D) NMR spectroscopy provides important information about the spatial proximity between host and guest atoms via observation of intermolecular dipolar cross-correlations. Two protons which are closely located in space can produce a nuclear Overhauser effect (NOE) cross-correlation between the relevant protons in NOESY or ROESY spectrum. The presence of NOE cross-peaks between protons from two species indicates spatial contacts within 0.4 nm. In order to gain more conformational information, 2D ROESY of the HP-β-CDs-thymol inclusion complexes was obtained and it is shown in Figure 6.

The ROESY spectrum of the HP-β-CDs-thymol complex showed appreciable correlation of the OH proton of thymol with the H-5 protons of HP-β-CDs and the T2" proton of thymol with the H-5 protons of HP-β-CDs (Figure 1 A, B). These results clearly indicate that thymol was included in the HP-β-CDs cavity.

Molecular Docking

To understand how thymol interacts with HP-β-CDs once complexed, docking simulations were carried out. Additionally, the structural information about the binding pose obtained by docking was shown in Figure 7, where thymol is observed to penetrate into the hydrophobic cavity of HP-β-CDs, detecting strong van der Waals interactions between the atoms of both molecules.

Figure 7C represents the view from the top of the complex (conical perspective), where thymol is shown in red, the atoms of the hydroxypropyl group of HP-β-CDs appear in blue, and the remaining atoms of HP-β-CDs are represented in green. The opposite view is shown in Figure 7D, where thymol is shown in red, the atoms of the hydroxypropyl group of HP-β-CDs in blue, and the other atoms of HP-β-CDs in green.

It is observed that thymol binds tightly into HP-β-CDs internal cavity. Hydrogens T2" from isopropyl group from thymol interact with hydrogen atoms H3 of HP-β-CDs (green sphere in figure 7A), and the hydrogen from hydroxyl group of thymol interacts with the atoms of hydrogen H5 of HP-β-CDs (purple sphere from figure 7A). The carbon atoms of the hydroxypropyl groups of HP-β-CDs are shown in light blue, while the remaining carbon atoms of HP-β-CDs are presented in green color (Figure 7B). These results agree with ^{1}H 2D-ROESY NMR data obtained (Figure 6). Also, it is clear that with this conformation, thymol binds tightly into HP-β-CDs hydrophobic core, if we have a look at the spheres representation of the molecules as shown in figure 7B, 7C and 7D.

Differential scanning calorimetry (DSC) and thermogravimetric analysis (TG)

Differential scanning calorimetry also was used for the recognition of inclusion complexes. When guest molecules are embedded into CDs cavities, their melting, boiling or sublimating points generally shifted to different temperature or disappeared. DSC and thermogravimetic analysis (TG) curves are shown in Figure 8.

The DSC curves of thymol presented three endothermic bands at about 50, 120 and 165-170 ºC. The first one is associated to its melting point (Figure 8A, a) and the rest which could be due to oxidation and volatilization of the chemical, with a 95% of mass reduction, as can be seen in TG analysis (Figure 8B, c). For HP-β-CDs, owing to its amorphous nature, a broad endothermic peak was observed approximately at 70 °C (Figure 8A, c) associated with its dehydration. An overall reduction of this signal is evident when thymol is complexed with CDs, suggesting a water exclusion process during complex formation (Figure 8A, b). The DSC curve of the HP-β-CDs-thymol complex (Figure 8A, b) did not exhibit the characteristic endothermic peaks of thymol

490 (Figure 8A, a), indicating that this compound was protected due to the formation of the
491 inclusion complex with HP-β-CDs.

492 The TG analysis (Figure 8, B) showed a different percentage of mass loss at 50
493 ºC, corresponding mainly to the water embedded into HP-β-CDs. The TG curve of HP-
494 β-CDs presented a weight loss of 5% (Figure 8B, a), and the HP-β-CDs-thymol curve had
495 a weight loss of 2.79% (Figure 8B, b). This situation suggests a water molecules reduction
496 in the internal cavity of HP-β-CDs due to the inclusion of thymol. Similar results were
497 observed in a previous study between thymol and β-CDs.[47]

498

499 **Fourier transform infrared spectroscopy (FT-IR)**

500 FTIR is a useful technique used to confirm the formation of an inclusion
501 complex.[48] The IR spectrum of HP-β-CDs (Figure 9) showed several peaks: 3341 cm^{-1}
502 (O-H stretching vibrations); 2923 cm^{-1}(C-H stretching vibrations); 1643 cm^{-1} (O-H
503 bending vibrations); 1157 cm^{-1}(C-O vibration); 1012 cm^{-1} (C–O–C stretching
504 vibrations); 850 cm^{-1}(α-type glycosidic bond); 2967 cm^{-1} (anti-symmetric vibration of
505 methyl groups); 1375 cm^{-1} (bending vibration of methyl).

506 The IR spectrum of thymol (Figure 9, inset), showed O-H stretching band at 3166
507 cm^{-1}, narrow peak of OH bending in plane at 1457 cm^{-1}, C=C aromatic stretching at 1621
508 cm^{-1}, 1585 cm^{-1}, and 1458 cm^{-1}; stretching C-H aromatic bend out of plane at 736 cm^{-1},
509 CH_3 symmetric and asymmetric stretching bands at 2866 and 2958 cm^{-1}, respectively,
510 and 804 cm^{-1} for out-of-plane CH wagging vibrations.The in plane C-H bending was
511 observed at 1089 cm^{-1} and 1058 cm^{-1}.

512 In the Figure 9, it should be noted that the bands of free thymol molecules were
513 generally covered up by the peaks of HP-β-CD-thymol complex because the quantities of
514 the guest molecules were no more than10–15 % (w/w) in the inclusion complexes.[49] The

two band of HP-β-CDs at 2923 and 2967 cm^{-1} corresponding to a C-H stretching vibrations and anti-symmetric vibration of methyl groups, respectively, were slightly shifted to 2925 and 2965 cm^{-1} and they have greater intensity. Moreover, the peak of C=C aromatic stretching of thymol at 1621 cm^{-1} appears in the HP-β-CDs-thymol complex shifted at 1619 cm^{-1}. This slight shifts relative to those of the respective free compounds, providing an evidence of host-guest interactions.

CONCLUSIONS

In conclusion, the results obtained in the stability study support the use of the MWI method in the preparation of solid HP-β-CD-thymol complexes, with a contact time of 24 h, due to the greater efficiency of encapsulation, but also other technological and economic advantages of great interest for industrial applications, such as process escalation at industrial level, or cost reduction (energy and labor saving). Moreover, MWI allows a rapid reaction heating without overheating the product, speeding up the process kinetics. The different characterization techniques have demonstrated the affinity of HP-β-CDs to thymol molecules, forming stable complexes.

ACKNOWLEDGEMENT

This work was supported by the Research, Development and Innovation Program oriented to the Challenges of the Society, within the framework of the State Plan for Scientific and Technical Research and Innovation 2013-2016, (RTC-2015-3321-2) and the Fundación Séneca (Agencia Regional de Ciencia y Tecnología, Región de Murcia) under grant 18946/JLI/13 and by the Nils Coordinated Mobility under grant 012-ABEL-CM-2014A (Malaga and CIEMAT).

REFERENCES

1. Sell C, Chemistry of essential oils, in *Handbook of Essential Oils: Science, Technology and Applications*, ed. by Başer KH and Buchbauer G. CRC Press, Boca Raton (Florida, USA), pp. 121–150 (2010).

2. Bilia AR, Guccione C, Isacchi B, Righeschi C, Firenzuoli F and Bergonzi MC, Essential oils loaded in nano systems: a developing strategy for a successful therapeutic approach. *Evidence-Based Complementary and Alternative Medicine* **651593:**1-14 (2014).

3. Vunda SLL, Sauter IP, Cibulski SP, Roehe PM, Bordignon SAL, Rott MB, Apel MA and von Poser GL, Chemical composition and amoebicidal activity of *Croton pallidulus*, *Croton ericoides*, and *Croton isabelli* (Euphorbiaceae) essential oils. *Parasitol Res* **111:**961–966 (2012).

4. da Cruz L, Pinto VF and Patriarca A, Application of plant derived compounds to control fungal spoilage and mycotoxin production in foods. *Int J Food Microbiol* **166:**1–14 (2013).

5. Elizaquível P, Azizkhani M, Aznar R and Sánchez G, The effect of essential oils on norovirus surrogates. *Food Control* **32:**275–278 (2013).

6. Gautam N, Mantha AK and Mittal S, Essential oils and their constituents as anticancer agents: a mechanistic view. *Bio Med Res Int* **2014:**1-23. (2014).

7. Liju VB, Jeena K and Kuttan R, Chemopreventive activity of turmeric essential oil and possible mechanisms of action. *Asia Pac J Cancer Prev* **15:**6575–6580 (2013).

8. Arranz E, Jaime L, de las Hazas ML, Reglero G and Santoyo S, Supercritical fluid extraction as an alternative process to obtain essential oils with anti-inflammatory properties from marjoram and sweet basil. *Ind Crop Prod* **67:**121–129 (2015).

564 9. Sheikh BA, Pari L, Rathinam A and Chandramohan R, Trans-anethole, a terpenoid
565 ameliorates hyperglycemia by regulating key enzymes of carbohydrate metabolism
566 in streptozotocin induced diabetic rats. *Biochimie* **112:**57–65 (2015).
567 10 Silva F and Domingues FC, Antimicrobial activity of coriander oil and its
568 effectiveness as food preservative. *Crit Rev Food Sci* **57:**35-47 (2015).
569 11. Licata M, Tuttolomondo T, Dugo G, Ruberto G, Leto C, Napoli EM, Rando R, Rita
570 Fede M, Virga G and Leone R, Study of quantitative and qualitative variations in
571 essential oils of Sicilian oregano biotypes. *J Essent Oil Res* **27:**293–306 (2015).
572 12. Mancini E, Senatore F, Del Monte D, De Martino L, Grulova D, Scognamiglio M,
573 Snoussi M and De Feo V, Studies on chemical composition, antimicrobial and
574 antioxidant activities of five *Thymus vulgaris* L. essential oils. *Molecules* **20:**12016–
575 12028 (2015).
576 13. Sarwar A and Latif Z, GC–MS characterisation and antibacterial activity evaluation
577 of Nigella sativa oil against diverse strains of Salmonella. *Nat Prod Res* **29:**447–
578 451 (2015).
579 14. Marchese A, Orhan IE, Daglia M, Barbieri R, Di Lorenzo A, Nabavi SF, Gortzi O,
580 Izadi M and Nabavi SM, Antibacterial and antifungal activities of thymol: A brief
581 review of the literature. *Food Chem* **210:**402–414 (2016).
582 15. Jaafari A, Tilaoui M, Mouse HA, M'bark LA, Aboufatima R, Chait A, Lepoivre M
583 and Zyad A, Comparative study of the antitumor effect of natural monoterpenes:
584 relationship to cell cycle analysis. *Rev Bras Farmacogn* **22:**534–540 (2012).
585 16. Deb DD, Parimala G, Devi SS and Chakraborty T, Effect of thymol on peripheral
586 blood mononuclear cell PBMC and acute promyelotic cancer cell line HL-60.
587 *Chem-bio Interac* **193:**97–106 (2011).

588 17. Yin Q, Yan F, Zu XY, Wu Y, Wu X, Liao M, Deng S, Yin L and Zhuang Y, Anti-
589 proliferative and pro-apoptotic effect of carvacrol on human hepatocellular
590 carcinoma cell line HepG-2. *Cytotechnology* **64:**43–51 (2012).
591 18. Llana-Ruiz-Cabello M, Gutiérrez-Praena D, Puerto M, Pichardo S, Jos Á and
592 Cameán AM, In vitro pro-oxidant/antioxidant role of carvacrol, thymol and their
593 mixture in the intestinal Caco-2 cell line. *Toxicol in Vitro* **29:**647–656 (2015).
594 19. Lai WW, Yang JS, Lai KC, Kuo CL, Hsu CK, Wang CK, Chang CY, Lin JJ, Tang
595 NY and Chen PY, Rhein induced apoptosis through the endoplasmic reticulum
596 stress, caspase-and mitochondria- dependent pathways in SCC-4 human tongue
597 squamous cancer cells. *In Vivo* **23:**309–316 (2009).
598 20. Marques HM, A review on cyclodextrin encapsulation of essential oils and
599 volatiles. *Flavour Frag J* **25:**313–326 (2010).
600 21. Ponce-Cevallos PA, Buera MP and Elizalde BE, Encapsulation of cinnamon and
601 thyme essential oils components (cinnamaldehyde and thymol) in β-cyclodextrin:
602 effect of interactions with water on complex stability. *J Food Eng* **99:**70–75 (2010).
603 22. Nieddua M, Rassua G, Boattoa G, Bosib P, Trevisib P, Giunchedia P, Cartaa A and
604 Gavini E, Improvement of thymol properties by complexation with cyclodextrins:
605 In vitro and in vivo studies. *Carbohyd Polym* **102:**393–399 (2014).
606 23. Glenn GM, Klamczynski AP, Imam SH, Chiou B, Orts WJ and Woods DF,
607 Encapsulation of plant oils in porous starch microspheres. *J Agric Food Chem*
608 **58:**4180–4184 (2010).
609 24. Guarda A, Rubilar JF, Miltz J and Galotto MJ, The antimicrobial activity of
610 microencapsulated thymol and carvacrol. *Int J Food Microbiol* **146:**144–150
611 (2011).

612 25. Meunier JP, Cardot JM, Gauthier P, Beyssac E and Alric M, Use of rotary
613 fluidized-bed technology for development of sustained-release plant extracts
614 pellets: Potential application for feed additive delivery. *J Anim Sci* **84:**1850–1859
615 (2006).
616 26. Higueras L, López-Carballo G, Cerisuelo JP, Gavara R and Hernández-Muñoz P,
617 Preparation and characterization of chitosan/HP-β-cyclodextrins composites with
618 high sorption capacity for carvacrol. *Carbohyd Polym* **97:**262–268 (2013).
619 27. Del Toro-Sánchez C, Ayala-Zavala J, Machi L, Santacruz H, Villegas-Ochoa M,
620 Alvarez-Parrilla E and González-Aguilar G, Controlled release of antifungal
621 volatiles of thyme essential oil from β-cyclodextrin capsules. *J Incl Phenom Macro*
622 **67:**431–441 (2010).
623 28. Higuchi T and Connors KA, Phase solubility techniques. *Adv Anal Chem Instrum*
624 **4:**56-63 (1965).
625 29. Hernández-Sánchez P, López-Miranda S, Guardiola L, Serrano-Martínez A,
626 Gabaldón JA and Nuñez-Delicado E, Optimization of a method for preparing solid
627 complexes of essential clove oil with β-cyclodextrins. *J Sci Food Agr* **97:**420-426
628 (2017).
629 30. Morris GM, Huey R, Lindstrom W, Sanner MF, Belew RK, Goodsell DS and Olson
630 AJ, AutoDock4 and AutoDockTools4: Automated docking with selective receptor
631 flexibility. *J Comput Chem* **30:**2785−2791 (2009).
632 31. Trott O and Olson AJ, Auto Dock Vina: Improving the speed and accuracy of
633 docking with a new scoring function, efficient optimization, and multithreading. *J*
634 *Comput Chem* **31:**455− 461 (2010).

635 32. Li R, Quan P, Liu D, Wei F, Zhang Q and Xu Q, The influence of co-solvent on
636 the complexation of HP-β-cyclodextrins with oleanolic acid and ursolic acid. *AAPS*
637 *Pharm Sci Tech* **10:**1137-1144 (2009).
638 33. Loftsson T and Hreinsdóttir D, The complexation efficiency. *J Incl Phenom Macro*
639 **57:** 545-552 (2007).
640 34 Kappe CO, Controlled microwave heating in modern organic synthesis. *Angew*
641 *Chem Int Ed* **43:**6250–6284 (2004).
642 35. Reineccius TA, Reineccius GA and Peppard TL, Encapsulation of flavors using
643 cyclodextrins: comparison of flavor retention in alpha, beta, and gamma types. *J*
644 *Food Sci* **67:**3271–3279 (2002).
645 36. Jaafari SM, Assadpoor E, He Y and Bhandari B, Encapsulation efficiency of food
646 flavours and oils during spray drying. *Dry Technol* **26:**816–835 (2008).
647 37. Wu Y, Zou L, Mao J, Huang J and Liu S, Stability and encapsulation efficiency of
648 sulforaphane microencapsulated by spray drying. *Carbohyd Polym* **102:**497–503
649 (2014).
650 38. Fernandes RV, Borges SV and Botrel DA, Gum arabic/starch/maltodextrin/inulin
651 as wall materials on the microencapsulation of rosemary essential oil. *Carbohyd*
652 *Polym* **101:**524–532 (2014).
653 39. Loksuwan J, Characteristics of microencapsulated β-carotene formed by spray
654 drying with modified tapioca starch, native tapioca starch and maltodextrin. *Food*
655 *Hydrocolloid* **21:**928–935 (2007).
656 40. Frascareli EC, Silva VM, Tonon RV and Hubinger MD, Effect of process
657 conditions on the microencapsulation of coffee oil by spray drying. *Food Bioprod*
658 *Process* **90:**413–424 (2012).

659 41. Alvarenga D, Vilela S, Fernandes R, Viana A, Gomes J and Marques G, Evaluation
660 of spray drying conditions on properties of microencapsulated oregano essential oil.
661 *Int J Food Sci Technol* **47:**2289–2296 (2012).
662 42. Medina-Torres L, Santiago-Adame R, Calderas F, Gallegos-Infante JA, González-
663 Laredo RF, Rocha-Guzmán NE, Núñez-Ramírez DM, Bernad-Bernad MJ and
664 Manero O, Microencapsulation by spray drying of laurel infusions
665 (*Litseaglaucescens*) with maltodextrin. *Ind Crop Prod* **90:**1–8 (2016).
666 43. Arpagaus C and Schafroth N, Spray drying of biodegradable polymers in laboratory
667 scale. *Resp Drug Deliv Eur* **2009:**269–74 (2009).
668 44. Tonon RV, Brabet C and Hubinger MD, Influence of process conditions on the
669 physicochemical properties of açai (*Euterpe oleraceae* Mart.) powder produced by
670 spray drying. *J Food Eng* **88:**411– 418 (2008).
671 45. Bergese P, Colombo I, Gervasoni D and Depero LE, Microwave generated
672 nanocomposites for making insoluble drugs soluble. *Mat Sci Eng C* **23:**791–795
673 (2003).
674 46. Mohit V, Harshal G, Neha D, Vilasrao K and Rajashree H, A comparative study of
675 complexation methods for cefdinir-hydroxypropyl-β-cyclodextrinsystem. *J Incl*
676 *Phenom Macro* **71:**57–66 (2011).
677 47. Fernandes LP, Éhen Z, Moura TF, Novák C and Sztatisz J, Characterization of
678 lippies idoides oil extract β-cyclodextrin complexes using combined
679 thermoanalytical techniques. *J Thermal Anal Calorim* **78:**557–573 (2004).
680 48. Ahmed SM, Naggi A, Guerrini M and Focher B, Inclusion complexes of
681 bropirimine with b-cyclodextrin in solution and in solid state. *Int J Pharmaceut*
682 **77:**247–254 (1991).

683 49. Yang Y and Song LX, Study on the inclusion compounds of eugenol with α-, β-,
684 γ- and Heptakis (2, 6-di-O-methyl)-β-cyclodextrins. *J Incl Phenom Macro* **53:**27–
685 33 (2005).
686
687
688
689
690
691
692
693
694
695
696
697
698
699
700
701
702
703
704
705
706

Table 1. Aqueous solubility (S_0), complexation constant (Kc), correlation coefficient of the phase solubility diagram (r^2), complexation efficiency (CE) and molar ratio of thymol for α-, β- and HP-β-CDsat different pH. ±SD. Standard deviation of triplicate diagrams.

	pH	S_0 (mmol L^{-1})	Kc (L mol^{-1})	r^2	CE (%)	Molar ratio
α-CD	3.5	6.42±0.20	281±26	0.971	39.9±5.0	1:4
	5.5	6.19±0.15	336±22	0.998	40.0±4.0	1:4
	6.5	6.02±0.12	600±54	0.991	61.2±10.1	1:3
	7.0	5.54±0.11	701±90	0.992	37.8±5.2	1:4
	8.5	5.92±0.10	592±97	0.993	54.5±0.12	1:3
β-CD	3.5	6.42±0.20	701±39	0.960	79.0±11.0	1:2
	5.5	6.19±0.15	866±19	0.944	71.9±13.0	1:2
	6.5	6.02±0.12	913±80	0.987	67.7±12.0	1:2
	7.0	5.54±0.11	1184±115	0.988	63.9±10.6	1:3
	8.5	5.92±0.10	580±45	0.988	53.3±9.1	1:3
HP-β-CD	3.5	6.42±0.20	291±19	0.988	41.3±6.0	1:3
	5.5	6.19±0.15	493±37	0.987	58.6±7.0	1:3
	6.5	6.02±0.12	638±73	0.997	65.0±5.0	1:3
	7.0	5.54±0.11	2583±176	0.999	139.5±12.3	1:2
	8.5	5.92±0.10	778±64	0.994	71.6±8.0	1:2

Table 2. ^{1}H-NMR Chemical Shifts (δ) of thymoland HP-β-CD, in the free and complexed forms, in D_2O.

	H-Atom	δ ppm^{-1} (Free)	δ ppm^{-1} (Complexed)	Δδ (Complexed - Free) ppm^{-1}
Thymol	H-C (3)	6.967	6.968	-0.001
	H-C (4)	6.573	6.575	-0.002
	H-C (6)	6.560	6.551	0.009
	H-C (2')	3.265	3.274	-0.009
	H-C (5')	2.197	2.202	-0.005
	H-C (2'')	1.169	1.172	-0.003
HP-β-CD	H-C (1)	5.074	5.070	0.004
	H-C (2)	3.723	3.726	-0.003
	H-C (3)	3.947	3.945	0.002
	H-C (4)	3.418	3.416	0.002
	H-C (5)	3.534	3.532	0.002
	H-C (6)	3.821	3.817	0.004
	H-C (9)	1.126	1.125	0.001

Molecular structure and atom numbering for thymol and HP-β-CD monomer are depicted in Figure 1 (A-B).

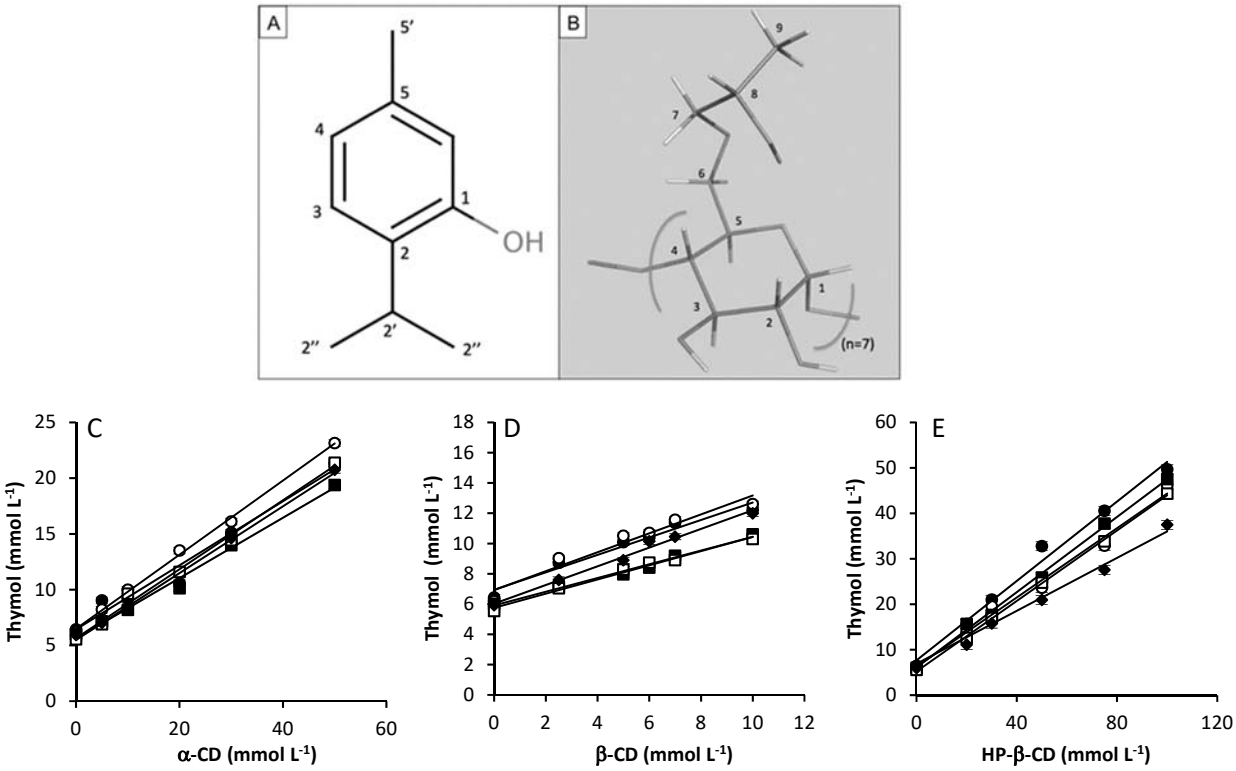

Figure 1. Molecular structure and atom numbering for thymol(A) and HP-β-CD monomer (B). Phase solubility diagrams of thymol with α-CDs (C), β-CDs (D) and HP-β-CDs (E) at pH 3.5 (●), pH 5.5 (○), pH 6.5 (■), pH 7.0 (□) and pH 8.5 (♦). Values represent means of triplicate determination.

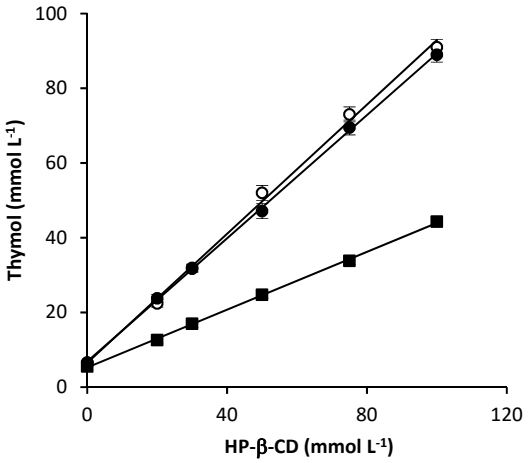

Figure 2. Phase solubility diagrams of thymol with HP-β-CD a pH 7.0 using the solubility method (■), the microwave method 24h MWI (○) and 48h MWI (●). Values represent means of triplicate determination.

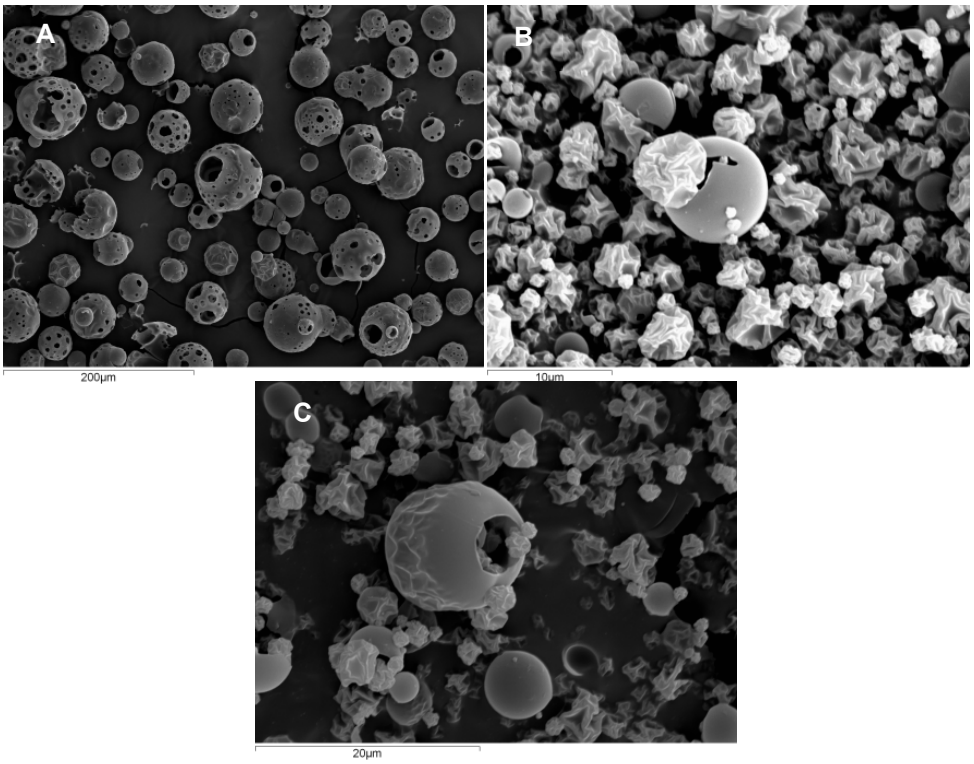

Figure 3. Microphotographs of HP-β-CDs (A), MWI method complexes (B) and solubility method complexes (C).

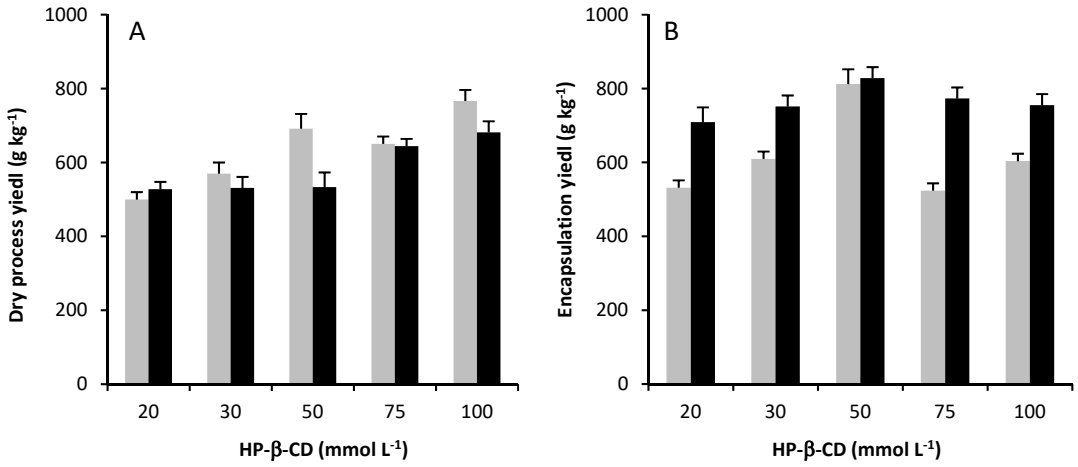

Figure 4: Drying process yield (A) (g kg^{-1}) and encapsulation yield of thymol (B) (g kg^{-1}) of HP-β-CDs-thymol complexes prepared by solubility method (grey bars) and MWI method (black bars).Values represent means of triplicate determination.

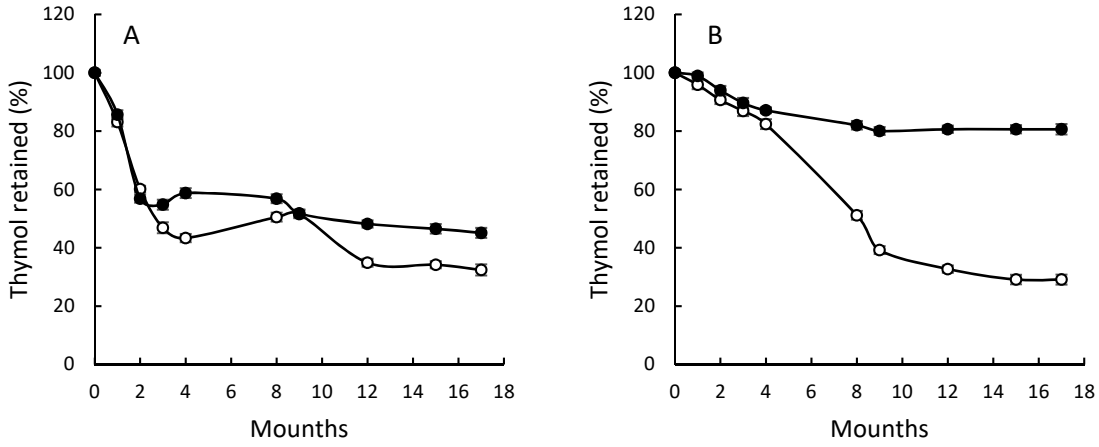

Figure 5. Evolution of thymol retained in solid complexes during 17 months of the storage at 4 ºC (○) and 25ºC (●). Complexes prepared by solubility method (A) and MWI method (B).Values represent means of triplicate determination.

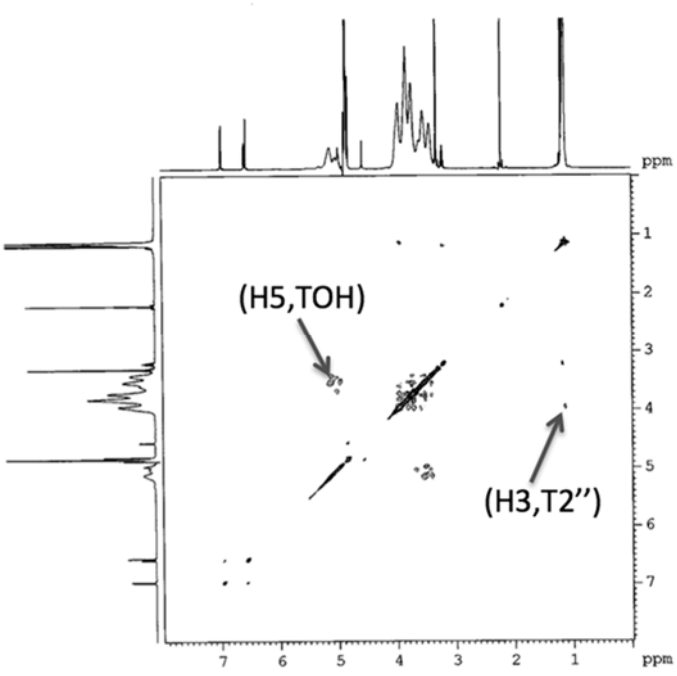

Figure 6. Evolution ROESY spectrum of HP-β-CDs-thymol complex in D_2O.

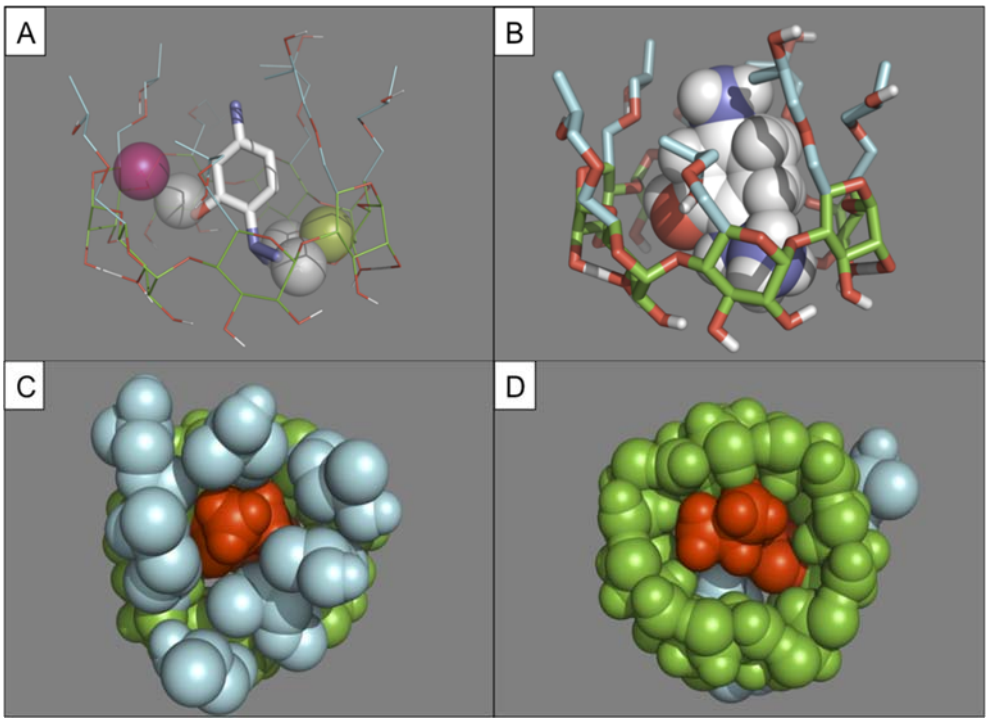

Figure 7: 3D perspectives of thymol and HP-β-CDs complexes obtained by molecular docking.

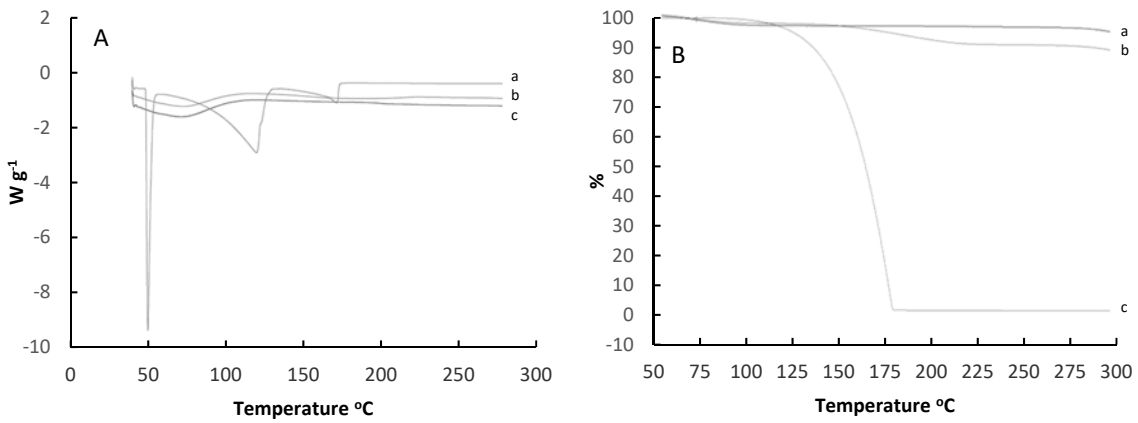

Figure 8: (A): DSC curves of a) thymol (pink); b) MWI HP-β-CDs-thymol (red); c) HP-β-CDs (green); (B): TG curves of a) HP-β-CDs (green); b) MWI HP-β-CDs-thymol (pink); c) thymol (blue).

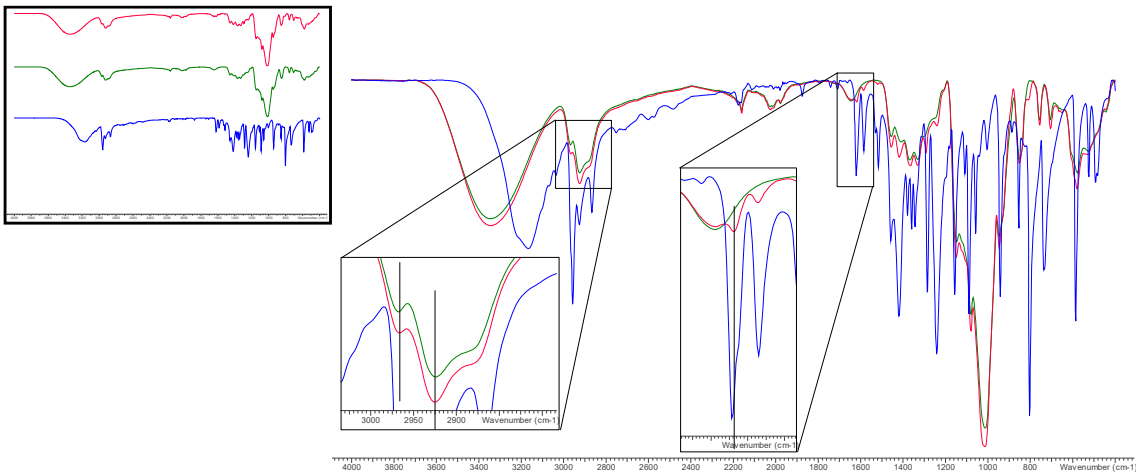

903

904 Figure 9: Inset: FTIR spectra of HP-β-CDs (green), HP-β-CDs-thymol (red) and thymol

905 (blue). Stacked FTIR spectra of HP-β-CDs (green), HP-β-CDs-thymol (red) and thymol

906 (blue). Vertical lines are indicating the maximum of HP-β-CDs-thymol curve.

907

908